recycling

MDPI

Article

Transforming Waste into Sustainable Construction Materials: Resistant Geopolymers from Recycled Sources

Rosalia Maria Cigala [1], Georgia Papanikolaou [1], Paola Lanzafame [1], Giuseppe Sabatino [2,3], Alessandro Tripodo [2], Giuseppina La Ganga [1], Francesco Crea [1], Ileana Ielo [1,*] and Giovanna De Luca [1,*]

[1] Department of Chemical, Biological, Pharmaceutical and Environmental Sciences, University of Messina, Viale F. Stagno d'Alcontres, 31-98166 Messina, Italy; rosaliamaria.cigala@unime.it (R.M.C.); georgia.papanikolaou@unime.it (G.P.); paola.lanzafame@unime.it (P.L.); giuseppina.laganga@unime.it (G.L.G.); francesco.crea@unime.it (F.C.)
[2] Department of Mathematical and Computer Sciences, Physical Sciences and Earth Sciences, University of Messina, Viale F. Stagno d'Alcontres, 31-98166 Messina, Italy; giuseppe.sabatino@unime.it (G.S.); alessandro.tripodo@unime.it (A.T.)
[3] National Institute of Oceanography and Experimental Geophysics, Via dei Mille, 28-98057 Milazzo, Italy
* Correspondence: ileana.ielo1@unime.it (I.I.); giovanna.deluca@unime.it (G.D.L.)

Abstract: The construction industry faces a growing challenge in managing waste materials, making the development of sustainable alternatives critical. This study investigates the preparation of geopolymers using construction and demolition waste materials, such as cement, brick, and glass waste. Specifically, crushed glass was used to produce sodium silicate, a key source of silicate ions and alkali necessary in geopolymerization processes. The performance of this in-house activator was compared to that of the commercial counterpart. Seven geopolymer formulations were prepared and characterized using SEM-EDX, ATR-FTIR, and XRD techniques. Chemical resistance against harsh environments was assessed through a 7-day immersion in water, hydrochloric acid (pH ~ 1), and sodium hydroxide (pH ~ 13) solutions. The samples were then dried and weighed to determine mass loss, revealing the promising resistance of specific formulations. Similarly, Portland cement specimens of the same dimensions as the geopolymer ones were prepared, tested, and compared to the geopolymers. Our study emphasizes the potential of transforming waste materials into high-performance, resistant geopolymers for construction materials. By optimizing waste-derived geopolymers, we may achieve significant environmental benefits through waste recycling and contribute to advancing sustainable construction technology.

Keywords: geopolymers; waste recycling; sustainability; circular economy; alkaline activated materials

Academic Editor: Huijuan Dong

Received: 25 March 2025
Revised: 25 April 2025
Accepted: 12 June 2025
Published: 14 June 2025

Citation: Cigala, R.M.; Papanikolaou, G.; Lanzafame, P.; Sabatino, G.; Tripodo, A.; La Ganga, G.; Crea, F.; Ielo, I.; De Luca, G. Transforming Waste into Sustainable Construction Materials: Resistant Geopolymers from Recycled Sources. *Recycling* **2025**, *10*, 118. https://doi.org/10.3390/recycling10030118

1. Introduction

The construction industry stands as a major contributor to global waste generation, with the accumulation of construction and demolition debris (C&D) posing a significant environmental challenge [1]. This ever-increasing waste volume necessitates a fundamental shift towards sustainable practices, driving research and development into innovative, eco-friendly construction materials [2]. Among these promising alternatives, geopolymers have emerged as a compelling substitute for traditional cement-based materials, offering a pathway to significantly reduce the industry's carbon footprint and mitigate the environmental impact associated with C&D waste [2]. Geopolymers, formed through the alkali activation of aluminosilicate precursors, present a versatile platform for utilizing a wide

range of source materials. These precursors can be derived from naturally occurring minerals, industrial by-products such as fly ash and slag, and, importantly, components of C&D waste like crushed concrete, brick, ceramic tile, and glass [2–8]. The geopolymerization process involves the reaction of these aluminosilicate materials with an alkaline activating solution, forming a dense and durable material that is often highly resistant [9].

Numerous studies have explored the feasibility of incorporating various waste materials into geopolymer production, investigating their influence on the resulting material's mechanical properties (compressive and flexural strength), durability (resistance to chemical attack, freeze-thaw cycles), and overall performance [10–15]. Researchers have experimented with different combinations of waste streams, optimizing mix designs, varying activator concentrations, and adjusting curing conditions (temperature, humidity) to achieve desired material characteristics tailored to specific applications. For instance, studies have investigated the use of fly ash-based geopolymers for structural elements, slag-based geopolymers for pavements, and waste glass-based geopolymers for decorative applications. Furthermore, the development of activators derived from waste materials, such as employing waste glass to produce sodium silicate solutions, has gained increasing attention, further enhancing the sustainability and circularity of geopolymer production [16]. Life Cycle Assessments (LCA) are increasingly crucial in evaluating the holistic environmental impact of geopolymer materials, being compared to traditional cement to provide a comprehensive framework for guiding the development of truly sustainable construction solutions [17]. These assessments consider the entire material life cycle, from raw material extraction and processing to manufacturing, use, and end-of-life disposal or recycling.

While existing research has extensively investigated the use of waste materials in geopolymer synthesis, a critical gap remains in the comprehensive utilization of exclusively waste-derived components, spanning from the aluminosilicate source to the activating solution. The reliance on commercially produced chemicals for activation limits the full potential for waste valorization and the realization of a truly circular economy. Achieving a 100% waste-derived geopolymer would represent a significant step towards greater sustainability. Despite incorporating waste materials as the primary aluminosilicate source, many studies still rely on commercially produced chemicals in the activation process. For instance, while waste glass might be used to produce the silicate solution, the precursor material to be activated is often metakaolin [6], a commercially processed clay mineral. In other cases, waste may be used as a precursor, but they are activated with commercial sodium silicate or require high curing temperatures ($T > 150\ ^{\circ}C$). This reliance on virgin materials, even in limited quantities, reduces the full potential for waste valorization and the realization of a truly circular economy within the construction sector.

This study aims to address this critical gap by focusing on developing geopolymers derived entirely from waste materials, effectively closing the loop on material flows. We explore the production of geopolymers using a carefully selected combination of waste cement and crushed brick as the primary aluminosilicate sources. These materials are readily available in C&D waste streams and offer diverse chemical compositions crucial for successful geopolymerization. We report on developing and thoroughly characterizing a novel, entirely waste-derived activator. This novel activator utilizes crushed glass waste to produce sodium silicate, a key component in the geopolymerization process. This approach aims to close the loop on material flows by using waste glass, another abundant component of C&D waste, to create the necessary alkaline environment for geopolymerization. Developing a reliable method to produce sodium silicate from waste glass on-site or regionally could significantly reduce the cost and environmental impact associated with transporting and using commercially produced activators. The resulting geopolymers are then tested to assess

their chemical resistance under harsh environmental conditions. This assessment includes exposure to highly acidic and alkaline solutions simulating challenging scenarios to evaluate their potential for practical applications in various construction contexts, thus showing the feasibility of producing high-performance geopolymers entirely from waste materials.

This research aims to advance sustainable construction practices significantly, contribute to a circular economy, and pave the way for a more environmentally responsible built environment by demonstrating the feasibility of producing high-performance geopolymers entirely from waste materials.

2. Results and Discussions

2.1. Chemical Resistance Tests

Water, acid, and alkali resistance are important durability properties in construction materials [9,10], and their effects were investigated in this research work. Table 1 presents the weight loss for each sample, including commercial Portland cement, following immersion in tap water, 0.1 M HCl, and 0.1 M NaOH. At the same time, Figure 1 illustrates the average sample mass after immersion, normalized to the average initial mass (see Figure S1 for the average absolute masses).

Table 1. Percentage weight loss of Samples 1–7 and commercial Portland cement after 7-day immersion in tap water, HCl, and NaOH.

Sample	% Weight Loss After 7-Day Immersion in		
	Tap Water	**HCl (0.1 mol/dm^3)**	**NaOH (0.1 mol/dm^3)**
1	0.29 ± 0.09	2.57 ± 0.02	1.74 ± 0.08
2	0.19 ± 0.08	1.90 ± 0.02	1.12 ± 0.07
3	0.25 ± 0.01	2.96 ± 0.01	1.92 ± 0.05
4	0.17 ± 0.06	1.77 ± 0.01	1.17 ± 0.06
5	0.26 ± 0.10	2.39 ± 0.02	1.88 ± 0.07
6	0.12 ± 0.07	1.18 ± 0.02	1.11 ± 0.05
7	0.30 ± 0.10	2.34 ± 0.01	1.74 ± 0.04
Portland cement	0.26 ± 0.05	5.66 ± 0.01	1.97 ± 0.08

Uncertainties as average absolute deviations.

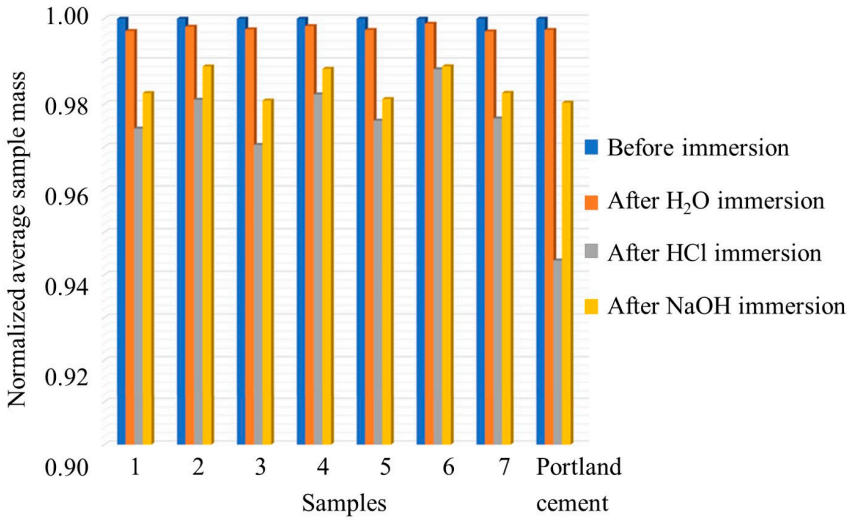

Figure 1. Average sample mass after immersion in tap water, 0.1 M HCl, and 0.1 M NaOH normalized for the average initial mass.

Sample 6, comprising 50 wt% of brick waste (B) and 20 wt% cement waste (C) geopolymerized with glass-derived silicate, exhibits the lowest weight loss (0.12%) in tap water

immersion, indicating the highest resistance among the tested samples. In contrast, Sample 7, which has the same composition but is geopolymerized with commercial silica, shows the highest weight loss (0.30%) in water, indicating the lowest resistance. Portland cement displays a weight loss of 0.26%, comparable to most geopolymeric samples, except Sample 6, which outperforms it.

In HCl, Sample 6 demonstrates the highest resistance, with a weight loss of 1.18%. Sample 3, produced from brick waste geopolymerized with commercial silica, exhibits the highest weight loss (2.96%) in this environment, indicating the greatest vulnerability to acidic conditions. Portland cement showed a weight loss of 2.66%, higher than most geopolymer samples except Sample 3, suggesting greater susceptibility to acid attack than the other geopolymeric materials. In fact, the orange coloring in Figure 2 indicates the formation of iron(III) oxide at the specimen surface, which may be attributed to the surface migration of Fe(III) ions from the tetracalcium aluminoferrite within the Portland cement clinker.

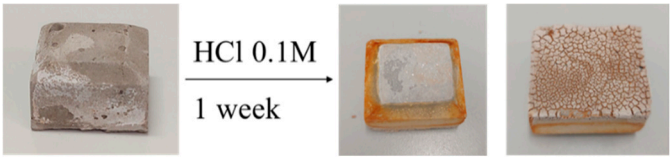

Figure 2. Photographs of a Portland cement sample after 7-day immersion in 0.1 M HCl.

Sample 6 again exhibits the lowest weight loss (1.11%) in NaOH, indicating strong resistance to alkali exposure. Conversely, Sample 3 shows the highest weight loss in NaOH (1.92%), consistent with its behavior in HCl, suggesting a generally lower resistance to harsh environments. Portland cement displays a weight loss of 1.97, exceeding most geopolymer samples, excluding Sample 3.

Given that Samples 2, 4, and 6 were produced using the same alkaline activator derived from glass waste, the differences in their chemical resistance could primarily stem from the variations in their precursor compositions (ratios of brick waste and cement waste) and the resulting Si/Al, Si/Na, Si/Ca, Si/K, Si/Mg, and Si/Fe mass ratios within the geopolymer matrix (Table 2).

Table 2. Si/M mass ratio (M = Al, Na, Ca, K, Fe, and Mg).

Sample	Si/Al	Si/Na	Si/Ca	Si/K	Si/Fe	Si/Mg
B	2.48 ± 0.04	25.50 ± 0.15	2.48 ± 0.10	8.91 ± 0.16	4.45 ± 0.16	98.00 ± 0.52
C	1.41 ± 0.06	8.31 ± 0.35	1.71 ± 0.10	10.23 ± 0.27	5.54 ± 0.29	12.09 ± 0.13
2	1.94 ± 0.07	3.98 ± 0.08	3.63 ± 0.13	18.45 ± 0.66	8.12 ± 0.30	29.00 ± 0.17
4	1.75 ± 0.09	4.47 ± 0.11	1.34 ± 0.07	23.00 ± 0.60	9.47 ± 0.44	40.25 ± 0.28
6	1.81 ± 0.08	3.48 ± 0.08	3.13 ± 0.13	20.89 ± 0.47	7.23 ± 0.29	26.86 ± 0.17

Uncertainties as average absolute deviations.

Despite its Si/Al ratio of 1.8 falling within the range of Samples 2 (1.93) and 4 (1.75), Sample 6, composed of a specific blend of 50 wt% brick and 20 wt% cement, demonstrated the best performance in chemical resistance, highlighting the complex interplay of various elemental ratios. While not exhibiting the highest Si/Al ratio, the ratio in Sample 6 may represent a more optimal balance for the alkali activation conditions provided by the glass-derived activator, potentially leading to a well-polymerized network with a favorable balance of durability, unlike less stable or more soluble gel structures that can result from excessively high or low ratios [9,18]. Among the three samples activated with the same glass-derived activator, Sample 6 presented the lowest Si/Na ratio (3.48), which can contribute to a higher density of negatively charged aluminate and silicate species, resulting

in a more tightly bound network due to enhanced electrostatic interactions with sodium ions, thus hindering the penetration of aggressive H^+ and OH^- ions [19]. With a Si/Ca ratio of 3.13, intermediate to Samples 2 and 4, the balanced calcium content in Sample 6 likely contributed to a denser microstructure by filling pores and potentially forming bridging structures without compromising the aluminosilicate network's integrity [20]. Similarly, the Si/K ratio of 20.89 in Sample 6, situated between the ratios of the other two samples, in conjunction with sodium, may have resulted in a more stable and less leachable alkali aluminosilicate gel, as the type and concentration of alkali cations influence the geopolymer matrix's stability in aggressive environments [21]. The intermediate Si/Mg ratio of 26.85 in Sample 6 suggests a balanced presence of magnesium that might have contributed to denser phase formation or positively influenced the gel structure for chemical resistance [8]. Finally, the Si/Fe ratio of 7.23 in Sample 6, again intermediate to the other two samples, indicates a moderate iron content that might have positively influenced the polymerization process or surface properties, potentially enhancing resistance to aggressive solutions, unlike the iron-related degradation observed in Portland cement exposed to HCl [22]. Therefore, the superior chemical resistance of Sample 6 might be due to a synergistic effect of a more optimized balance across multiple elemental ratios resulting from its specific precursor blend and its interaction with the glass waste-derived activator.

Overall, samples produced using glass waste-derived silicate demonstrate greater immersion resistance than those fabricated with commercial sodium silicate or Portland cement under identical conditions.

2.2. Characterizations

The following studies focus on the characterization of samples produced by alkalinization with waste glass-derived silicate.

Figure 3 displays ATR-FTIR spectra recorded for the geopolymeric Samples 2, 4, and 6, all made with SG, the noise observed in the spectral region between 2500 and 2000 cm^{-1} being probably due to instrumental interference. The characteristic bands are summarized in Table 3 and are in agreement with the literature on similar geopolymerized samples [23,24].

Table 3. ATR-FTIR characteristic bands.

Sample	**Band Position (cm^{-1})**		
2	3160	1424	998
4	3240	1408	968
6	3204	1424	968
Characteristic bands	O-H stretching	O-C-O stretching	Si-O-Si and Si-O-Al stretching
References	[25]	[11]	[26,27]

The spectra of Samples 2, 4, and 6 (Figure 3) show characteristic bands (Table 3) around 3160–3240 cm^{-1}, 1408–1424 cm^{-1}, and 968 cm^{-1}. The bands around 3160–3240 cm^{-1} can be attributed to O-H stretching, indicating the presence of hydroxyl groups, likely from residual water or structural OH within the geopolymer matrix [25]. The bands in the 1408–1424 cm^{-1} range correspond to O-C-O stretching, suggesting the presence of carbonate species, which can arise from atmospheric carbon dioxide reacting with alkaline components in the geopolymer [11]. The prominent band at around 968 cm^{-1} can be assigned to Si-O-Si and Si-O-Al stretching vibrations, which are the primary indicators of the geopolymerization process, signifying the formation of the aluminosilicate gel network [26,27]. These FTIR results align with the observed chemical resistance. The presence of a well-formed aluminosilicate network contributes to the material's ability to withstand aggressive chemical attack. Sample 6, which demonstrated the

best chemical resistance, also exhibits these characteristic bands, suggesting a denser and more stable geopolymer structure.

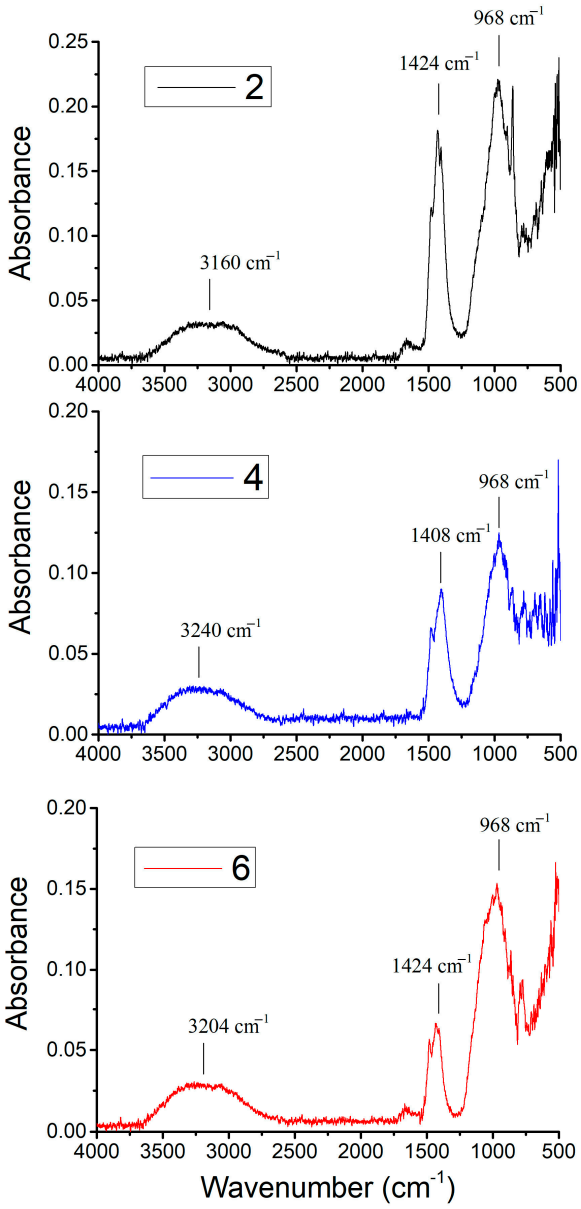

Figure 3. ATR-FTIR spectra of Samples 2, 4, and 6.

Figure 4 shows the X-ray diffractograms of Samples 2, 4, and 6, which were geopolymerized using SG. These Diffractograms indicate the presence of quartz, calcite, portlandite, and wollastonite phases, consistent with literature data for similar geopolymers produced with commercial silicates [28]. Comparison with the diffractograms of the starting waste-derived matrices (Figure 5) reveals the formation of portlandite and wollastonite crystalline phases upon geopolymerization, as these phases are absent in brick and cement waste. While B (Figure 5, blue line) exhibits diopside and quartz phases, Sample 2, where B is the only aluminosilicate matrix, also shows portlandite and calcite [25]. Quartz is likely derived from the original waste materials, as it is a common mineral in both cement and brick. Calcite can form due to carbonation during the geopolymerization process or sample storage, while portlandite and wollastonite are products of the alkali activation and subsequent reactions. The formation of these crystalline phases provides further insight into the chemical resistance of the geopolymers. For instance, the presence of wollastonite,

a calcium silicate mineral, can contribute to improved mechanical properties and chemical stability. As suggested by XRD, the absence of significant amounts of highly soluble phases in Sample 6 correlates with its superior performance in the chemical resistance tests.

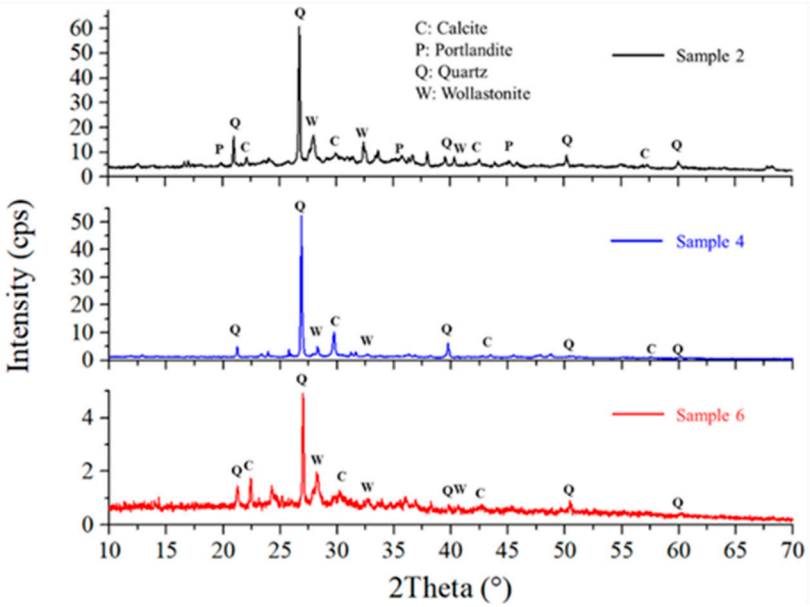

Figure 4. XRD Patterns and mineral phase of geopolymer 2, 4, and 6.

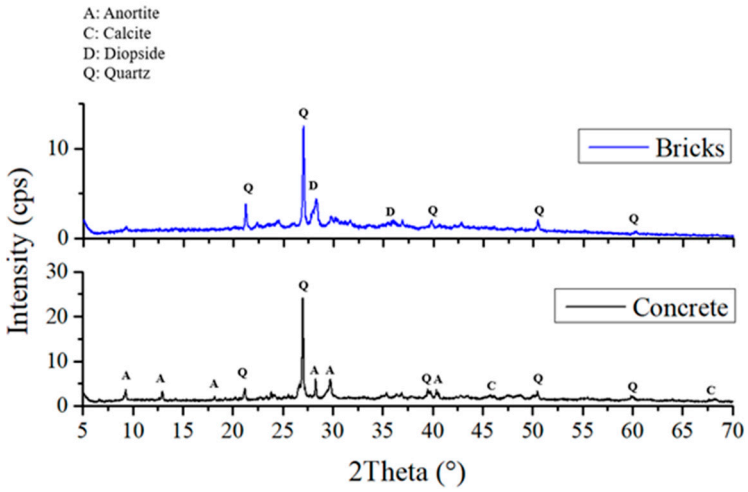

Figure 5. XRD Patterns and mineral phase of bricks and Portland cement wastes.

Scanning Electron Microscopy (SEM) micrographs are recorded to examine the microstructural changes in waste-derived precursors following geopolymerization with glass-derived silicate (Figure 6). Sample 4 exhibits a compact, flaky structure, which is also observed in Samples 2 and 6. These latter samples also show that unreacted or partially reacted glass materials are incorporated into their structure. Pristine brick waste (Figure 7) presents characteristics of a vitreous morphology, probably forming during kiln firing and not due to geopolymerization, which occurs at room temperature. Table 4 summarizes the results of the EDX elemental analyses of the rectangular regions shown in the SEM micrographs presented in Figure 6 and 7. Table 4 summarizes the EDX elemental analyses of the rectangular regions in the SEM micrographs shown in Figures 6 and 7. The Si/M ratios presented in Table 2 were calculated according to the results of the EDX elemental analysis. Microstructural and chemical composition changes were observed in Samples 2, 4, and 6 compared to the precursors. SEM images reveal a compact and flaky microstructure

in all three samples, indicating the formation of a dense geopolymer matrix. The presence of unreacted or partially reacted glass particles suggests that the geopolymerization process may not have fully consumed all the precursor materials. However, providing a heterogeneous structure can also contribute to the material's overall stability. The vitreous morphology of the pristine brick waste is a result of the high-temperature firing process used in brick production. This structure is distinct from the geopolymer matrix formed at room temperature, highlighting the microstructural transformation achieved through alkali activation.

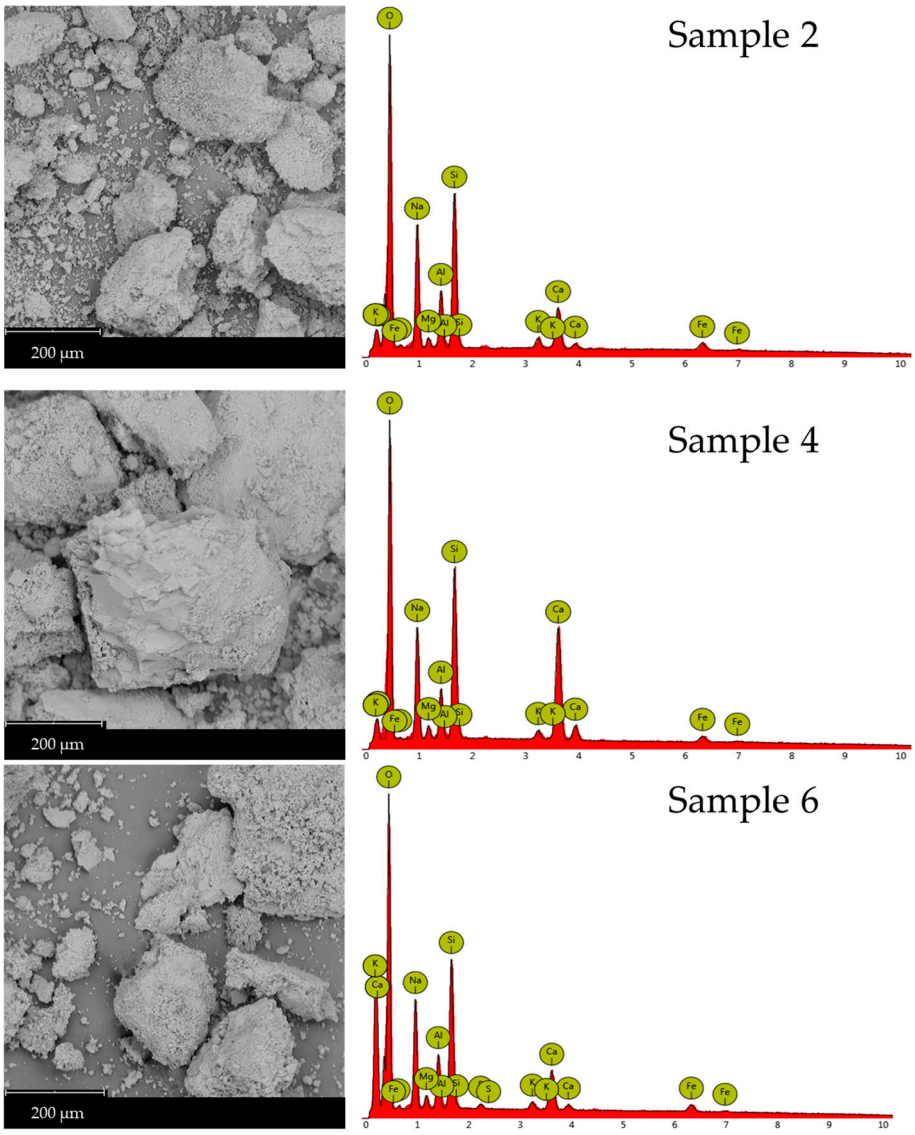

Figure 6. SEM micrographs (left column) and EDX analysis (right column) of Samples 2, 4, and 6 (first, second, and third row, respectively).

As shown in Figure 6 and detailed in Table 4, the EDX spectra of the geopolymers revealed an increased percentage of silicon, aluminum, and calcium, confirming the presence of wollastonite and portlandite, which was previously established by XRD. Additional SEM micrographs of the samples, captured at varying magnifications, are presented in Figures S2–S4.

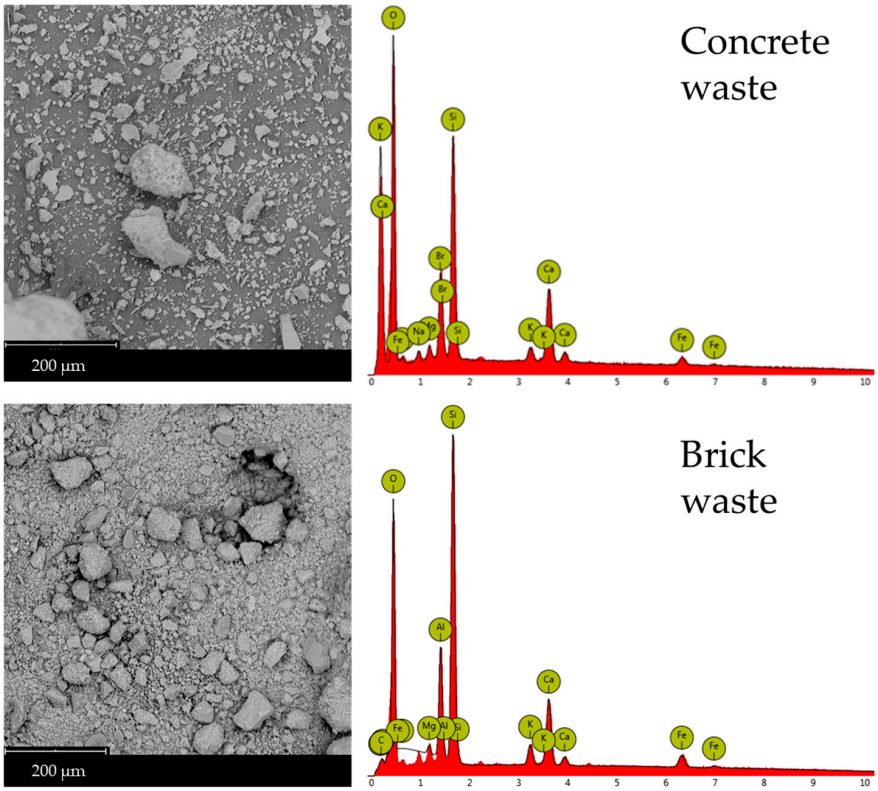

Figure 7. SEM micrographs and EDX Analysis of concrete and brick waste.

Table 4. Quantitative EDX analysis results (expressed as atomic mass percentages) of the samples corresponding to the presented SEM micrographs presented.

Symbol Element	B	C	2	4	6
O	57.0 ± 0.8	63.0 ± 0.9	54.1 ± 0.9	56.4 ± 0.9	55.4 ± 0.9
Si	19.6 ± 0.4	13.3 ± 0.5	20.3 ± 0.5	16.1 ± 0.5	18.8 ± 0.5
Al	7.9 ± 0.2	9.4 ± 0.2	10.5 ± 0.5	9.2 ± 0.5	10.4 ± 0.6
Na	0.8 ± 0.1	1.6 ± 0.5	5.1 ± 0.3	3.6 ± 0.3	5.4 ± 0.3
Ca	7.9 ± 0.6	7.8 ± 0.5	5.6 ± 0.6	12.0 ± 0.5	6.0 ± 0.6
K	2.2 ± 0.3	1.3 ± 0.3	1.1 ± 0.7	0.7 ± 0.4	0.9 ± 0.4
Fe	4.4 ± 0.6	2.4 ± 0.6	2.5 ± 0.7	1.7 ± 0.7	2.6 ± 0.7
Mg	0.2 ± 0.1	1.1 ± 0.1	0.7 ± 0.1	0.4 ± 0.1	0.7 ± 0.1

Uncertainties as standard deviations.

The EDX data presented in Table 4 were acquired from area scans corresponding to the SEM micrographs shown in Figures 6 and 7. EDX analysis supports the XRD findings, showing an increase in silicon (Si), and aluminum (Al) content in Sample 6 compared to the starting materials. This increase confirms the formation of the aluminosilicate gel and calcium-containing phases like wollastonite and portlandite. The elemental composition, particularly the Si/Al and Si/Ca ratios, plays a crucial role in determining the geopolymer's properties. Sample 6, with its specific elemental ratios (as discussed in Section 2.1), exhibits a microstructure that contributes to its enhanced chemical resistance.

3. Materials and Methods

3.1. Materials

Commercial Portland cement, construction cement (C), and hollow clay brick (B) waste were supplied by the construction company Procori srl (Catania, Italy) and were used as raw materials. Waste cement and brick materials were crushed using a ball mill for 60 min

and sieved through 500 µm sieves. Dusty glass waste was supplied by the glazier A. Scarfì and F. D'Arrigo (Messina, Italy), and it was used to produce the alkaline activator solution. The manufacturer provided the glass directly in powder form; therefore, it was only sieved through 50 µm sieves before use. Silicate standard solution, sodium hydroxide, hydrochloric acid, hydrofluoric acid, ultrapure water, ammonium molybdate, ascorbic acid, oxalic acid, and glycerin were purchased at VWR (Milan, Italy), and sodium silicate was purchased at Ingessil s.r.l. (Verona, Italy). All chemicals were used without any further purification.

3.2. Preparation of Sodium Silicate from Glass Waste

Sodium silicate was prepared from dusty glass waste ("Silicate from Glass", SG) by adding 120 g SG to sodium hydroxide pellets to obtain sodium silicate with molar ratios of SiO_2/Na_2O and H_2O/Na_2O equal to 0.5 and 10, respectively [6,26]. The mixture was mixed with 700 cm^3 of water for 2 h using a magnetic stirrer to enhance the dissolution of silica. The exothermic effect of the solubilization of sodium hydroxide caused an increase in the suspension's temperature, which was thermally isolated to exploit the spontaneous heating favoring silica dissolution. Before being used, the suspension was stored for at least one week to allow complete silica solubilization/equilibration [6] and to decant the supernatant from the undissolved glass powder. The resulting solution was used as an alkaline activator for the geopolymerization reaction, with an aliquot being reserved for the quantitative analysis of silica.

3.3. Sodium Silicate Solution Titration

The silica-molybdenum blue reaction, with ascorbic acid as the reducing agent, was employed to establish a reliable method for determining sodium silicate content [29]. The standard solutions and samples were analyzed spectrophotometrically. 1 cm^3 of acidified ammonium molybdate solution (8.38 mM), 5 cm^3 of oxalic acid 5% (m/V), 1 cm^3 of ascorbic acid 0.04 mol/dm^3, 1 cm^3 of glycerin 1% (v/v), and purified water (up to 50 mL total volume) were mixed, the resulting solution being used as blank. The above-described conditions were also used to prepare standard sodium silicate solutions (final concentrations: 0.1 to 1.5 mg/dm^3), and the aliquot (10 mL) of the above-described SG dissolution to be analyzed. All solutions were left in polyethylene bottles for 20 min to develop a blue color.

The absorbance at λ = 818 nm for the standard (Figure 8, black squares) and unknown (Figure 8, red dot) samples were measured in 1 cm PMMA cuvettes against the blank solution. The unknown silicate concentration was determined against the obtained calibration curve, obtaining a value of (6.72 ± 0.15) mg/dm^3.

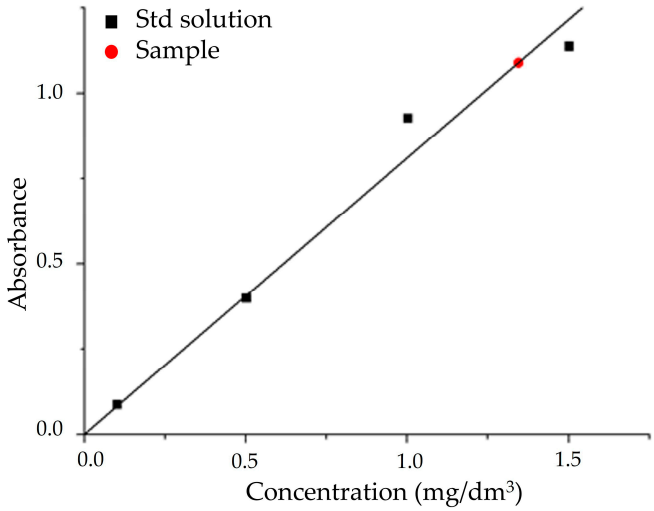

Figure 8. Calibration curve for the quantitative determination of sodium silicate in SG sample.

3.4. Geopolymer Samples Preparation

Raw materials C and B were crushed and ground using a laboratory crusher and a ball mill, the resulting powders being sieved through a chrome-plated mesh sieve with a 0.45 mm aperture size.

Seven geopolymer samples were prepared with compositions, reported in Table 5 as mass % and kg/m^3, designed to verify the successful geopolymerization under various conditions. This design accounts for the inherent heterogeneity of construction waste materials collected without distinguishing between bricks and cement, thus simulating potential real-world waste combinations.

Table 5. Geopolymers composition.

Sample	Mixture (w/w% ‖ kg/m^3)		Commercial Sodium Silicate (w/w% ‖ kg/m^3)	SG (w/w% ‖ kg/m^3)
	C	B		
1	70 ‖ 1925	-	-	30 ‖ 825
2	-	70 ‖ 2052	-	30 ‖ 879
3	-	70 ‖ 2292	30 ‖ 982	-
4	50 ‖ 1475	20 ‖ 590	-	30 ‖ 885
5	50 ‖ 1530	20 ‖ 612	30 ‖ 859	-
6	20 ‖ 634	50 ‖ 1584	-	30 ‖ 950
7	20 ‖ 769	50 ‖ 1923	30 ‖ 1154	-

The symbol "‖" is used as separators for the two measurements.

The precursors were mixed in a domestic mixer for 30 min and subsequently poured into silicone molds with a volume of 7.57 cm^3, calculated for a solid composed of a rectangular prism and a truncated pyramid. They were left to cure covered in sealed vessels at room temperature to inhibit carbonation.

Similarly, commercial Portland cement specimens with the same dimensions as the geopolymer ones were prepared for comparison by mixing cement powder with water and subsequent air drying.

Figure 9 shows the seven geopolymeric specimens described in Table 5, while Figure 10 shows a Portland cement specimen.

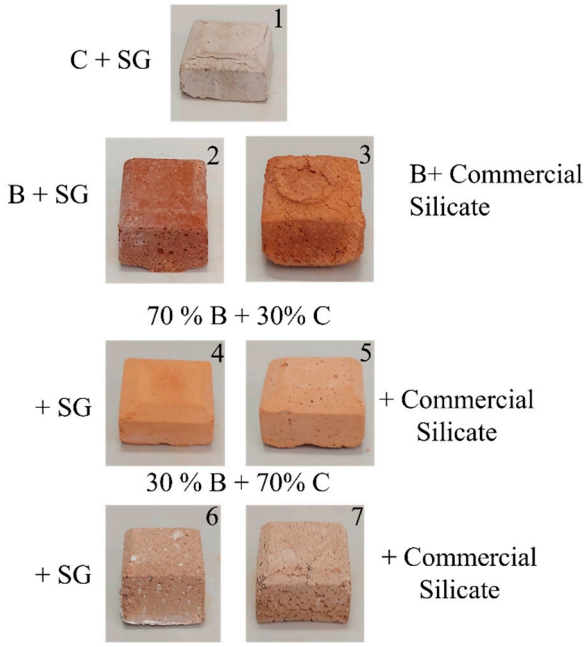

Figure 9. Samples of geopolymers labeled 1–7 and the relative compositions, as described in Table 5.

Figure 10. Commercial Portland cement sample.

3.5. Chemical Resistance Tests

Preliminary analysis of weight loss after immersion in water across three independent batches (3 samples per batch) demonstrated reasonable repeatability and reproducibility, with a 95% confidence interval for the mean weight loss of (0.21%, 0.36%), supporting the use of triplicate samples for the main experimental conditions.

Tests of the chemical resistance of geopolymers were performed in triplicates for the different compositions and environmental conditions. Individual 8 cm^3 samples were weighed and immersed for 7 days at room temperature (20 °C) in 1 dm^3 of:

- tap water, with pH = 8.12 ± 0.01 and Λ = (0.6 ± 0.1) mS cm^{-1}
- 0.1 M HCl solution, with pH = 1.03 ± 0.05 and Λ = (42.6 ± 0.1) mS cm^{-1}
- 0.1 M NaOH solution, with pH = 13.11 ± 0.07 and Λ = (23.3 ± 0.1) mS cm^{-1}

Following immersion, each specimen was dried in a ventilated oven at 60 °C overnight and weighed to determine mass loss. The pH of all solutions and the electrical conductivity of the tap water solutions were recorded. Mass loss, pH, and conductivity values were calculated as the measurements' average on the three replicate samples. The reported uncertainty represents the average absolute deviation.

The geopolymer cubes were finally crushed into thoroughly homogenized powder to be used for all other characterizations.

3.6. Characterizations

UV/vis spectrophotometric titrations were carried out on a Stellarnet BLACK-Comet-SR diode array spectrophotometer equipped with a combined deuterium/tungsten halogen lamp (Stellarnet mod. SL5) and a multimodal fiber optic cable (length: 1 m; diameter: 1 mm; optical range: 190–1100 nm).

The crystallinity and purity of synthesized phases were evaluated by X-ray powder diffraction (XRD) in the $5° < 2\theta < 70°$ region, with a step size of 0.025° s^{-1} and X-ray wavelength of 1.5406 Å (Bruker D2 Phaser).

Fourier Transform IR (FTIR) spectra were recorded in Attenuated Total Reflection (ATR) using a Thermo Scientific (Milan, Italy) spectrophotometer model iS50 ATR. The scans were performed at a resolution of 4 cm^{-1}, and the spectra were reported as absorbance vs. wavenumbers (cm^{-1}).

Samples' particle morphology, microstructure, and chemical composition were examined using a Phenom scanning electron microscope model ProX Desktop equipped with an Energy-Dispersive X-ray Spectroscopy probe (SEM-EDX). To this end, the powdered samples were deposited onto SEM stubs covered by a conductive carbon adhesive.

4. Conclusions

This study demonstrates the feasibility of transforming construction and demolition debris and glass waste into resistant, high-performance geopolymer-based construction

materials. The successful utilization of an in-house glass-derived sodium silicate activator validates its effectiveness as a sustainable alternative to commercial sodium silicate, embodying circular economy principles by closing the loop on material flows.

Geopolymer samples demonstrated promising chemical resistance under aggressive environmental conditions, including immersion in acidic and alkaline solutions. Notably, Sample 6 consistently exhibited the lowest weight loss across all immersion tests, signifying its superior resistance to water, acid, and alkali. This composition, incorporating brick waste and glass-derived silicate, outperformed both Portland cement and other geopolymer formulations. Conversely, Sample 3 exhibited the highest weight loss in both HCl and NaOH, indicating its lowest resistance to chemical attack.

Portland cement generally exhibited higher weight loss than most geopolymer samples, particularly in HCl and NaOH, indicating that geopolymeric materials may offer improved chemical resistance in specific environments. These findings highlight the potential for superior performance of select geopolymer formulations compared to traditional Portland cement, especially under chemically aggressive conditions.

Characterization techniques, including XRD, FTIR, and SEM-EDX, provided valuable insights into the mineralogical phase transformations, bonding mechanisms, and microstructural characteristics of the geopolymers. The formation of crystalline phases, such as wollastonite and portlandite, coupled with the development of a compact, flaky microstructure, suggests the potential for enhanced mechanical durability.

Building upon the findings related to chemical resistance, future research will extend to comprehensive mechanical property evaluation, essential for structural applications. Long-term durability studies are also planned to provide a complete understanding of material performance.

This research presents a sustainable and environmentally sound approach to construction by effectively utilizing waste materials and reducing reliance on traditional Portland cement. The demonstrated feasibility of producing high-performance construction materials from readily available waste streams offers a practical avenue to minimize environmental impact, conserve natural resources, and reduce greenhouse gas emissions associated with cement production. Furthermore, the development of a waste-derived activator enhances the sustainability of this methodology.

The enhanced chemical resistance of the developed geopolymer, particularly Sample 6, suggests its suitability for applications in harsh environments where traditional Portland cement may degrade prematurely. This includes:

- Construction in contaminated soils: Geopolymers can be used for foundations or underground structures in soils with high acidity or alkalinity, preventing structural damage.
- Industrial flooring: Geopolymers can withstand exposure to chemical spills and harsh cleaning agents in factories and warehouses.

To further advance the practical application of waste-derived geopolymers, future research should focus on:

- Mechanical properties: Comprehensive evaluation of compressive strength, flexural strength, and toughness to ensure structural integrity.
- Optimization of formulations: Further research into the ideal ratios of waste materials and activators to maximize performance and consistency.
- Durability studies: Long-term assessment of resistance to freeze-thaw cycles, abrasion, and UV exposure.
- Scale-up and production: Developing cost-effective methods for large-scale production of geopolymers from waste materials.
- Life Cycle Assessment (LCA): A detailed LCA to fully quantify the environmental benefits compared to traditional cement, including energy consumption and CO_2 emissions.

By addressing these areas, we can pave the way for the wider adoption of sustainable, waste-derived geopolymers in the construction industry, promoting a circular economy and reducing the environmental footprint of the built environment. This research aligns with broader efforts in materials science and engineering to develop innovative, resource-efficient solutions that meet societal demands while minimizing environmental impact and promoting a circular economy.

Supplementary Materials: The following supporting information can be downloaded at: https://www.mdpi.com/article/10.3390/recycling10030118/s1. Figure S1: Mass loss for Samples 1–7 and commercial Portland cement. Figure S2: SEM micrograph of Samples 2, 4, 6, B, and C at 100 µm scale and 840× magnification. Figure S3: Samples 2, 4, 6, B, and C at 50 µm scale and 1700× magnification. Figure S4: Samples 2, 4, 6, B, and C at 30 µm scale and 2700× magnification.

Author Contributions: Conceptualization: I.I.; Methodology: I.I., R.M.C., and G.D.L.; Investigation: G.P., P.L., and G.S.; Formal analysis: I.I. and G.L.G.; Visualization: I.I., A.T., and G.D.L.; Supervision: G.D.L. and F.C.; Project Administration: G.D.L.; Resources: G.D.L., A.T., G.S. and F.C.; Funding acquisition: G.D.L. and F.C.; Writing—original draft: I.I. and R.M.C.; Writing—review and editing: all authors. All authors have read and agreed to the published version of the manuscript.

Funding: This research received no external funding.

Data Availability Statement: The data supporting this article have been included as part of the Supplementary Materials.

Acknowledgments: The authors would like to thank Procori S.r.l. for donating construction materials and to A. Scarfi and F. D'Arrigo for providing the glass powder used in this study.

Conflicts of Interest: The authors declare no conflicts of interest.

Abbreviations

The following abbreviations are used in this manuscript:

C&D	Construction and demolition
C	Concrete waste
B	Hollow clay brick waste
SG	Glass waste-derived sodium silicate
PMMA	Poly(methyl methacrylate)
ATR-FTIR	Attenuated Total Reflectance—Fourier Transform Infrared Spectroscopy
XRD	X-Ray Diffraction
SEM-EDX	Scanning Electron Microscopy—Energy Dispersive X-Ray Spectroscopy

References

1. Giacobello, F.; Ielo, I.; Belhamdi, H.; Plutino, M.R. Geopolymers and Functionalization Strategies for the Development of Sustainable Materials in Construction Industry and Cultural Heritage Applications: A Review. *Materials* **2022**, *15*, 1725. [CrossRef]
2. Amran, Y.H.M.; Alyousef, R.; Alabduljabbar, H.; El-Zeadani, M. Clean production and properties of geopolymer concrete; A review. *J. Clean. Prod.* **2020**, *251*, 119679. [CrossRef]
3. Bakri, M.M.A.; Mohammed, H.; Kamarudin, H.; Niza, I.K.; Zarina, Y. Review on fly ash-based geopolymer concrete without Portland Cement. *J. Eng. Technol. Res.* **2011**, *3*, 1–4.
4. Lancellotti, I.; Piccolo, F.; Traven, K.; Češnovar, M.; Ducman, V.; Leonelli, C. Alkali Activation of Metallurgical Slags: Reactivity, Chemical Behavior, and Environmental Assessment. *Materials* **2021**, *14*, 639. [CrossRef]
5. Lancellotti, I.; Vezzali, V.; Barbieri, L.; Leonelli, C.; Grillenzoni, A. Construction and Demolition Waste (CDW) valorization in alkali activated bricks. In *Wastes: Solutions, Treatments and Opportunities III*; CRC Press: Boca Raton, FL, USA, 2019; ISBN 978-0-429-28979-8.
6. Tchakouté, H.K.; Rüscher, C.H.; Kong, S.; Kamseu, E.; Leonelli, C. Geopolymer binders from metakaolin using sodium waterglass from waste glass and rice husk ash as alternative activators: A comparative study. *Constr. Build. Mater.* **2016**, *114*, 276–289. [CrossRef]

7. Rahimpour, H.; Amini, A.B.; Sharifi, F.; Fahmi, A.; Zinatloo-Ajabshir, S. Facile fabrication of next-generation sustainable brick and mortar through geopolymerization of construction debris. *Sci. Rep.* **2024**, *14*, 10914. [CrossRef]
8. Ye, T.; Xiao, J.; Duan, Z.; Li, S. Geopolymers made of recycled brick and concrete powder—A critical review. *Constr. Build. Mater.* **2022**, *330*, 127232. [CrossRef]
9. Davidovits, J. Chemistry of geopolymeric systems, terminology. In *99 Geopolymer International Conference Proceedings*; Geopolymer Institute: Saint-Quentin, France, 1999; Volume 2, pp. 9–40.
10. Moudio, A.M.N.; Tchakouté, H.K.; Ngnintedem, D.L.V.; Andreola, F.; Kamseu, E.; Nanseu-Njiki, C.P.; Leonelli, C.; Rüscher, C.H. Influence of the synthetic calcium aluminate hydrate and the mixture of calcium aluminate and silicate hydrates on the compressive strengths and the microstructure of metakaolin-based geopolymer cements. *Mater. Chem. Phys.* **2021**, *264*, 124459. [CrossRef]
11. Ahmari, S.; Zhang, L. Durability and leaching behavior of mine tailings-based geopolymer bricks. *Constr. Build. Mater.* **2013**, *44*, 743–750. [CrossRef]
12. Ariffin, M.A.M.; Bhutta, M.A.R.; Hussin, M.W.; Mohd Tahir, M.; Aziah, N. Sulfuric acid resistance of blended ash geopolymer concrete. *Constr. Build. Mater.* **2013**, *43*, 80–86. [CrossRef]
13. Amran, M.; Huang, S.-S.; Debbarma, S.; Rashid, R.S.M. Fire resistance of geopolymer concrete: A critical review. *Constr. Build. Mater.* **2022**, *324*, 126722. [CrossRef]
14. Li, Q.-H.; Zhao, S.-Y.; Huang, B.-T.; Xu, L.-Y.; Xu, S.-L. Simultaneous enhancement of ductility and sustainability of high-strength Strain-Hardening Cementitious Composites (SHCC) using recycled fine aggregates. *J. Clean. Prod.* **2024**, *470*, 143357. [CrossRef]
15. El-Seidy, E.; Chougan, M.; Al-Noaimat, Y.A.; Al-Kheetan, M.J.; Ghaffar, S.H. The impact of waste brick and geo-cement aggregates as sand replacement on the mechanical and durability properties of alkali–activated mortar composites. *Results Eng.* **2024**, *21*, 101797. [CrossRef]
16. Bueno, E.T.; Paris, J.M.; Clavier, K.A.; Spreadbury, C.; Ferraro, C.C.; Townsend, T.G. A review of ground waste glass as a supplementary cementitious material: A focus on alkali-silica reaction. *J. Clean. Prod.* **2020**, *257*, 120180. [CrossRef]
17. Altimari, F.; Lancellotti, I.; Leonelli, C.; Andreola, F.; Elsayed, H.; Bernardo, E.; Barbieri, L. Green materials for construction industry from Italian volcanic quarry scraps. *Mater. Lett.* **2023**, *333*, 133615. [CrossRef]
18. Duxson, P.; Fernández-Jiménez, A.; Provis, J.L.; Lukey, G.C.; Palomo, A.; van Deventer, J.S.J. Geopolymer technology: The current state of the art. *J. Mater. Sci.* **2007**, *42*, 2917–2933. [CrossRef]
19. Springer Nature. *Alkali Activated Materials: State-of-the-Art Report, RILEM TC 224-AAM*; Provis, J.L., Van Deventer, J.S.J., Eds.; RILEM State-of-the-Art Reports; Springer: Dordrecht, The Netherlands, 2014; Volume 13, ISBN 978-94-007-7671-5.
20. García-Lodeiro, I.; Fernández-Jiménez, A.; Palomo, A. 17-Alkali-activated based concrete. In *Eco-Efficient Concrete*; Pacheco-Torgal, F., Jalali, S., Labrincha, J., John, V.M., Eds.; Woodhead Publishing Series in Civil and Structural Engineering; Woodhead Publishing: Sawston, Cambridge, 2013; pp. 439–487. ISBN 978-0-85709-424-7.
21. Bakharev, T.; Sanjayan, J.G.; Cheng, Y.-B. Resistance of alkali-activated slag concrete to acid attack. *Cem. Concr. Res.* **2003**, *33*, 1607–1611. [CrossRef]
22. Nath, S.K.; Kumar, S. Influence of iron making slags on strength and microstructure of fly ash geopolymer. *Constr. Build. Mater.* **2013**, *38*, 924–930. [CrossRef]
23. Giannetto, A.; Puntoriero, F.; Notti, A.; Parisi, M.F.; Ielo, I.; Nastasi, F.; Bruno, G.; Campagna, S.; Lanza, S. Self-assembly of hexameric macrocycles from PtII/ferrocene dimetallic subunits—Synthesis, characterization, chemical reactivity, and oxidation behavior. *Eur. J. Inorg. Chem.* **2015**, *2015*, 5730–5742. [CrossRef]
24. Chukanov, N.V.; Chervonnyi, A.D. *Infrared Spectroscopy of Minerals and Related Compounds*; Springer: Berlin/Heidelberg, Germany, 2016; ISBN 978-3-319-25349-7.
25. Vafaei, M.; Allahverdi, A.; Dong, P.; Bassim, N. Acid attack on geopolymer cement mortar based on waste-glass powder and calcium aluminate cement at mild concentration. *Constr. Build. Mater.* **2018**, *193*, 363–372. [CrossRef]
26. Part, W.K.; Ramli, M.; Cheah, C.B. An overview on the influence of various factors on the properties of geopolymer concrete derived from industrial by-products. *Constr. Build. Mater.* **2015**, *77*, 370–395. [CrossRef]
27. Zhang, M.; Zhao, M.; Zhang, G.; Mann, D.; Lumsden, K.; Tao, M. Durability of red mud-fly ash based geopolymer and leaching behavior of heavy metals in sulfuric acid solutions and deionized water. *Constr. Build. Mater.* **2016**, *124*, 373–382. [CrossRef]
28. Kogbara, R.B.; Al-Zubi, A.; Mortada, Y.; Hammoud, A.; Masad, E.A.; Khraisheh, M.K. Lime-activated one-part geopolymer mortars from construction, demolition and industrial wastes. *Results Eng.* **2024**, *21*, 101739. [CrossRef]
29. Yang, H.; Li, C.; Wei, C.; Li, M.; Li, X.; Deng, Z.; Fan, G. Molybdenum blue photometry method for the determination of colloidal silica and soluble silica in leaching solution. *Anal. Methods* **2015**, *7*, 5462–5467. [CrossRef]